

Southern Connecticut State University

**Finding and Analyzing the  $\Lambda$  and  $\bar{\Lambda}$  from Au + Au Nuclei Collisions at the Relativistic  
Heavy Ion Collider**

Thesis submitted to meet the requirements

for departmental honors in physics

by

**Richard Magnotti**

2017

**Finding and Analyzing the  $\Lambda$  and  $\bar{\Lambda}$  from Au + Au Nuclei Collisions at the Relativistic  
Heavy Ion Collider**

by

**Richard Magnotti**

This honors thesis was prepared under the direction of the candidate's thesis advisor, Dr. Evan Finch, Department of Physics and it has been approved by the members of the candidate's thesis committee. It was successfully defended and accepted by the University Honors Thesis Committee.

---

Dr. Evan Finch  
Thesis Advisor

---

Dr. Elliot Horch  
University Reader

---

Dr. Matthew Enjalran  
Second Reader

---

Dr. Matthew Enjalran  
Department Chairperson

---

Date

**Honors Thesis Defense Signature Sheet (HON 495 or HON 493)**

***Student Name:*** \_\_\_\_\_

***Honors Thesis Title:*** Finding and Analyzing the  $\Lambda$  and  $\bar{\Lambda}$  from Au + Au Nuclei Collisions at the Relativistic Heavy Ion Collider

***Date of Honors Thesis Defense:*** May 5 2017

***Signatures indicating approval of the Honors Thesis Defense:***

*Print name*

*Signature*

\_\_\_\_\_  
*Thesis Advisor*

\_\_\_\_\_  
*University Reader*

\_\_\_\_\_  
*Second Reader*

\_\_\_\_\_  
*Department Chairperson (if in attendance)*

***Thesis Abstract (Required):***

\_\_\_ *I have attached a copy of the abstract for this thesis.*

\_\_\_ *I have also e-mailed an electronic copy of this abstract to Dr. Finch at*

*finchl3@southernct.edu*

*This page intentionally left blank*

# **Finding and Analyzing the $\Lambda$ and $\bar{\Lambda}$ from Au + Au Nuclei Collisions at the Relativistic Heavy Ion Collider**

Thesis submitted to meet the requirements

for departmental honors in physics

by

**Richard Magnotti**

## **Abstract**

The goal of this experiment is to develop software to identify  $\Lambda$  particles from particle collisions. We will use the data from the RHIC (Relativistic Heavy Ion Collider) STAR (Solenoidal Tracker at RHIC) collaboration from Brookhaven National Laboratory. STAR is a particle detector built for use with the RHIC. Thus, the joint experiments done using both STAR and RHIC have been classified under the umbrella term the STAR collaboration. Our STAR collaboration experiment of interest involves the collisions of two Au particle beams which produce tens of thousands of particles as byproducts among which are  $\Lambda$  particles. However, the  $\Lambda$  quickly decays into a proton and  $\pi$ . Therefore, our software will examine these particles and discern protons and  $\pi$ s by measuring their end momentum and energy loss.

## Chapter 1

### Introduction

The Brookhaven RHIC is used to study the conditions that existed in the universe shortly after its creation, specifically something called *quark-gluon plasma* (QGP). In the first millionths of a second after the Big Bang only free quarks and gluons existed, no protons or neutrons, hence QGP. Then, once cooled, protons and neutrons were formed<sup>1</sup>. The way the RHIC recreates these conditions is by producing Au+Au nuclei collisions (center of mass energy of 200 GeV per nucleon)<sup>2</sup>. Two separate, large, rings move beams of heavy ions along the circular track in opposite directions until collision. The beams are accelerated by an electric field and directed along the path by a magnetic field. The collisions can have energies up to 250 GeV. Au nuclei are among the largest nuclei of the common elements, and thus create a larger region of QGP when collided.

The  $\Lambda$  is a neutral particle classified as a baryon, which means it's comprised of three smaller elementary particles called quarks (uds). The  $\Lambda$  decays into a combination of proton and  $\pi^-$ , whereas the  $\bar{\Lambda}$  (bar accent represents abbreviation for “anti-particle”) decays into an antiproton and  $\pi^+$  with a lifetime of  $\sim 2.6 \times 10^{-10}$  seconds. Protons are spin  $\frac{1}{2}$  particles also classified as baryons and comprised of three quarks ( $p$ :  $uud$ ,  $\bar{p}$ :  $\bar{u}\bar{u}\bar{d}$ ), while the  $\pi$  is a meson and thus comprised of a quark and antiquark ( $\pi^+$ :  $u\bar{d}$ ,  $\pi^-$ :  $d\bar{u}$ )<sup>2</sup>. The STAR particle detector was used to examine this  $\Lambda$  particle decay,  $\Lambda \rightarrow \pi^- p$ , and  $\bar{\Lambda} \rightarrow \pi^+ \bar{p}$ . This particle decay can be seen in figure 1. The Feynman diagram<sup>3</sup> as shown provides an in depth visual to explain the process of a neutral  $\Lambda$  decaying into the  $p$  and  $\pi^-$  by a subatomic force called the weak interaction (for the

purpose of this research the details of the weak interaction are unimportant). The main STAR detector that has provided the particle track data is the time projection chamber or TPC. The TPC records the particle tracks and allows us to determine pertinent information such as momenta and ionization energy loss ( $dE/dx$ )<sup>4</sup>. Utilizing remote access to the RHIC computational facility or RACF, data was accessed from the STAR collaboration experiment and examined.

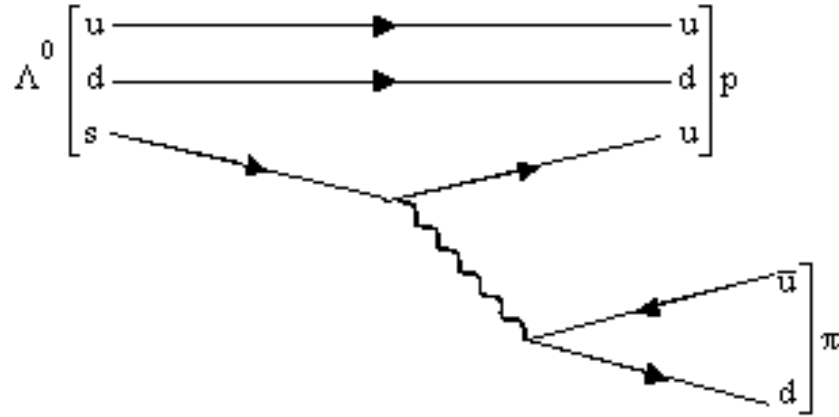


*Figure 1.  $\Lambda$  decay Feynman diagram*

## 1.1 Previous Work

It has been found that generally objects in nature are different than their mirror images. It seems as though nature has a preferred setup of objects' anatomies. Everything from organic specimens in the laboratory to humans exhibit chiral (handedness) asymmetry. Despite the fact that many things are chirally asymmetric, at one time it was thought that the four fundamental forces of nature were chirally symmetric. The four fundamental forces are the strong nuclear force (which holds nuclei together), gravitational force, electromagnetic force (which is responsible for interactions between charged particles), and weak force (which is responsible for radioactive decay). In 1956, Chien-Shiung Wu conducted an experiment that showed the weak force is in

fact not always parity invariant, and thus exhibited chirality. This means that on a fundamental level nature can discern left and right handed systems<sup>5</sup>.

If it is impossible for a particle or process' mirror image to exist, this is called parity violation. We are interested in the trend of parity violation in nature. For example, whether nature has a preference of left or right handed particles resulting from a decay or collision that has no chirality. Because the  $\Lambda$  decays by the weak interaction it does not follow the rules of parity – thus the  $\Lambda$  decay is chirally asymmetric<sup>6</sup>. The  $\Lambda$ , therefore, is of particular interest because its decay is so indicative of its chirality. Figure 2 shows a cartoon diagram of the decay of the  $\Lambda$  particle and the expected paths the daughter particles will take.

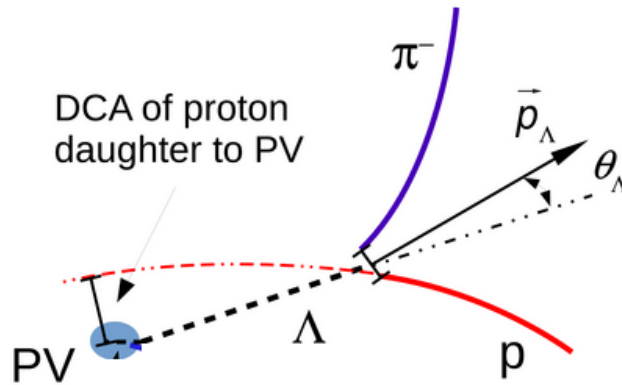


Figure 2. Diagram of  $\Lambda$  decaying into proton and  $\pi$



## Chapter 2

### Physics

#### 2.1 Methods

The goal of this experiment is to develop software to identify  $\Lambda$  particles from particle collisions. STAR is a particle detector built for use with the RHIC. Thus, the experiments done using both STAR and RHIC have been classified under the umbrella term the STAR collaboration. Our STAR collaboration experiment of interest involves the collisions of two gold particles each of which produces tens of thousands of particles as byproducts among which are expected to be several  $\Lambda$  particles. However, the  $\Lambda$  decays into a proton and  $\pi$  fairly quickly – with a mean lifetime of  $\sim 2.6 \times 10^{-10}$  seconds in which it travels a few centimeters. Therefore, our software will sift through these particles and discern protons and  $\pi$ s by measuring their end momentum and energy loss.

#### 2.2 Finding the $\Lambda$ Particles

The  $\Lambda$  is a neutral particle. Because it has no charge it cannot be examined directly because the time projection chamber is unable to identify neutral particles since they do not leave trails of ionized atoms behind. Therefore, it was our goal to determine which particles were products of the decay of the  $\Lambda$ . We examined the produced particles from Brookhaven National Laboratory's RHIC STAR collaboration. As the particles move away from the collision region in the TPC, they have a curved trajectory due to moving in the experiment's magnetic field. This is because of the Lorentz force,  $\vec{F}_B = q\vec{E} + q\vec{v} \times \vec{B}$  which essentially states that a particle of charge  $q$  will experience a force if moving through a magnetic field  $\vec{B}$  and electric field  $\vec{E}$  with velocity  $\vec{v}$ . As

they move, these produced particles “knock” out electrons from ions in the TPC gas as they pass through, leaving trails of free electrons behind that can then be collected by detectors at the ends of the TPC after being pushed to the ends by an electric field in the TPC<sup>7</sup>.

In the broader scheme, our goal is to test for parity violation of a particle collision. It is relatively easy to measure the handedness of  $\Lambda$ s, and this is why we are studying them specifically. “Handedness” or “helicity” defines the correspondence between a particle’s spin/angular momentum and the direction its moving. As can be seen in figure 3, we are presented the left and right hand rule. These can be distinguished by pointing your thumb in the direction of velocity of the particle, and the curling your fingers in the direction of the spin. Depending on which figure within the diagram the particle fits will dictate whether it is left or right handed. If the particle fits the diagram of the left hand the particle is left-handed, and vice-versa for right handed<sup>8</sup>. When  $\Lambda$ s decay, the resulting proton tends to have a preference to move in the same direction as the  $\Lambda$  spin in the  $\Lambda$  rest frame. Because we know the direction of  $\Lambda$  motion, we then only need to measure the spin of each particle in order to determine its helicity<sup>9</sup>. After determining which particles are in fact products of  $\Lambda$  decays, our software will compare all resultant particles from the collision and measure the helicity of each, then calculate the number of left versus right handed  $\Lambda$  decays. We will test for fluctuations of parity violation as opposed to a net violation. During the creation of the particles immediately post-collision, small instances of space may have a higher number of particles of a certain helicity. If we do find parity violation this means nature (at least in small instances) prefers one helicity over another. Aside from this being an interesting fact, brought to light is the question as to why the universe even has a general preference of helicity. The STAR experiment is designed to create conditions strikingly similar to the big bang.

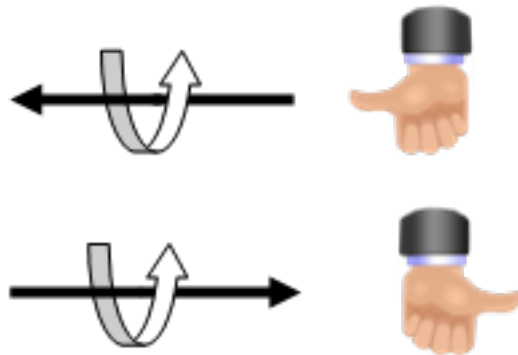


*Figure 3. Distinction between left (bottom) and right (top) handed particles*

### Chapter 3

## Facilities

### 3.1 RHIC

The RHIC is roughly 2.4 miles long, and can accelerate particles to speeds near the speed of light. The actual track along which the ions travel can be seen in figure 4. The process of the particle collision is different than what might be thought of as a typical particle collision. The actual process could be characterized classically as two small spherical objects hitting one another. However, because the particles are moving at relativistic speeds, they undergo relativistic effects such as Lorentz contraction. Lorentz contraction is the idea that from a rest frame, two moving objects moving near the speed of light will decrease in length from the point of view of the rest frame observer<sup>10</sup>. Therefore, the particle collisions in the RHIC can be thought of in the same way. The particles will appear as more flat objects than spheres, as can be seen by equation 1. In this equation,  $L$  is the observed length from rest frame,  $L'$  is the observed length of the moving frame,  $v$  is the velocity of the moving object, and  $c$  is the speed of light ( $3.0 \times 10^8$  m/s). Because the ions move at such high speeds ( $\sim 99.7\%$  the speed of light upon collision), the goal of the RHIC is to loosen the protons and neutrons in order to free the quarks and gluons inside<sup>11</sup>. As the matter cools down, thousands of resultant particles are created. Among these particles are  $\Lambda$ s, and post-decay, the protons and  $\pi$ s. A visual representation of the particle collision process can be seen below in figure 5 – figure 8.

$$L = L' \sqrt{1 - \frac{v^2}{c^2}} \quad (1)$$

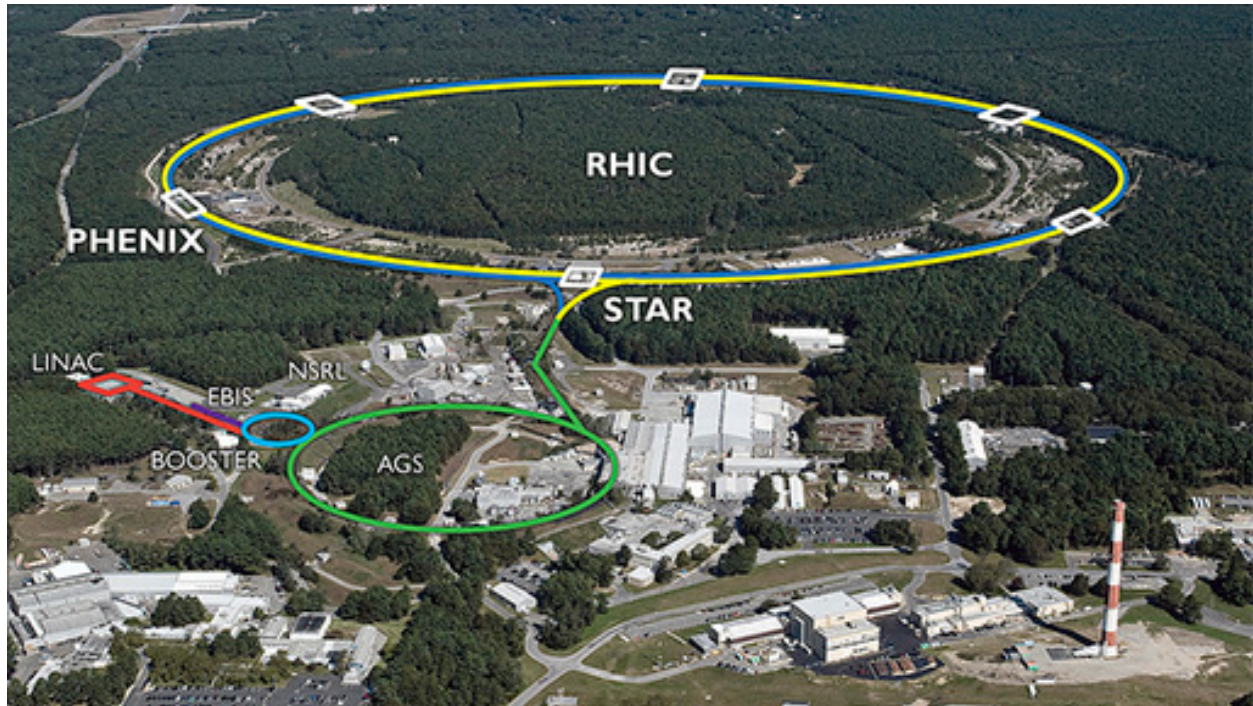


*Figure 4. Bird's-Eye View of the RHIC at Brookhaven National Laboratory*



*Figure 5. The two Lorentz contracted contracted particles moving towards each other<sup>7</sup>*

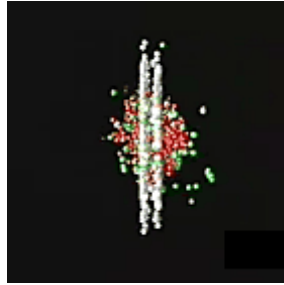


*Figure 6. Collision of the particles and release of the protons and neutrons<sup>7</sup>*

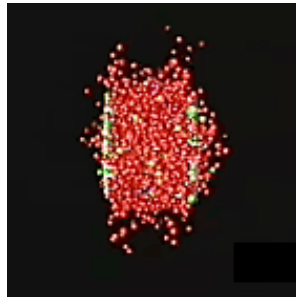


*Figure 7. Release of the quarks and gluons from the loosened protons and neutrons<sup>7</sup>*

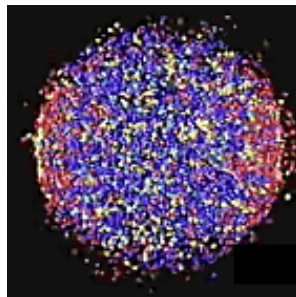


*Figure 8. Creation of the thousands of resultant particles as the matter cools off<sup>7</sup>*

### 3.1 STAR and TPC

STAR is a particle detector built for use with the RHIC. Thus, the experiments done using both STAR and RHIC have been classified under the umbrella term the STAR collaboration. The goal of the STAR detector is simply to record data regarding the collisions taking place in the RHIC<sup>12</sup>. Our STAR collaboration experiment of interest involves the collisions of two gold particles each of which produces tens of thousands of particles as byproducts among which are expected to be several  $\Lambda$  particles.

As they move, the particles produced from the STAR Au+Au collisions “knock” out electrons from atoms in the TPC gas as they pass through, leaving trails of free electrons behind that can then be collected by detectors at the ends of the TPC after being pushed to the ends by an electric field in the TPC<sup>13</sup>. This can be seen in figure 9. The incident particle in this case would be a resultant particle from the Au+Au collision. The figure should be viewed left to right, and shows an example of what the trail of ionized particles would look like as they drift from the cathode to the anode pads. Because the ionization creates a weak electron signal, through signal amplification it can be detected. As the particles move away from the collision region in the TPC, they have a curved trajectory due to the Lorentz force from moving in the experiment’s magnetic field<sup>14</sup>. Thus, based on the curvature of the track and the known strength of the applied B-field<sup>15</sup>, momentum can be calculated.

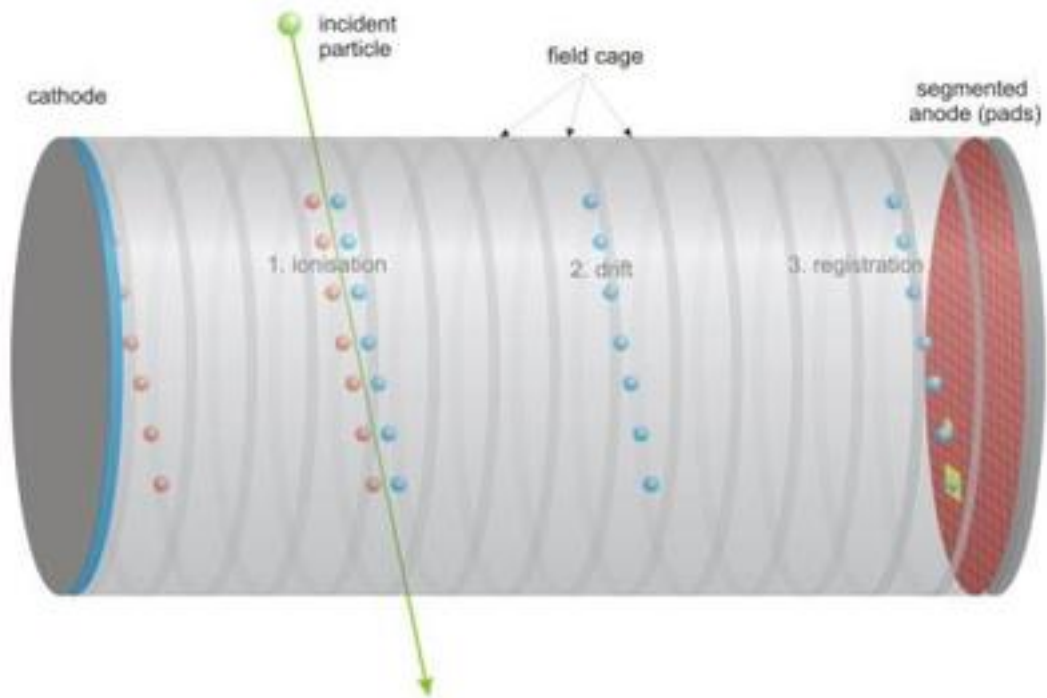


*Figure 9. The drift chamber and charged particles' movement as a result of the E-field*



## Chapter 4

### Methods of Implementation and Analysis

#### 4.1 What it Means to have a “Track”

The TPC records the particle “tracks”. We examined the produced particles from Brookhaven National Laboratory’s RHIC STAR collaboration. Figure 10 shows a visualization of tracks from an Au+Au collision event that actually took place in the TPC. The opening in the middle is the collision zone, where the particles actually collide. These collected free electrons hold all pertinent information about the charged particle that passed through<sup>14</sup>. The path of collected free electrons is recognized by pattern recognition software and a “track” representing this is created in the ROOT software.

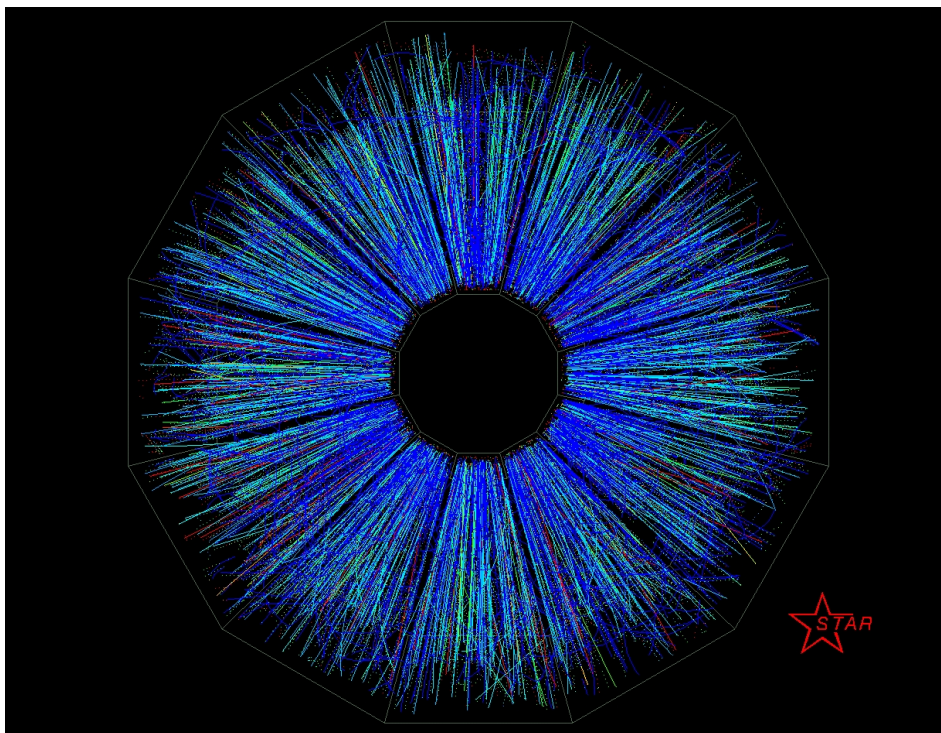


*Figure 10. The ionized gas particle trails left by the charged particle spray<sup>12</sup>*

## 4.2 General Approach to Implementation

Once the information on the particles was gathered, by remote access to the RACF the data was examined. The method of examination was C++ code which was then manipulated and added to. The particle tracks were sorted by their charge and the most likely particle type determined by the closest related particle energy loss. I created a list of particles likely to be protons and a separate list of particles most likely to be  $\pi$ s. The particles were then paired up with their respective corresponding anti-particle in such a way that each potential  $\pi^-$  is paired with each potential  $p$  (and  $\pi^+$  with  $\bar{p}$ ). The resultant histogram created an expected negative exponential curve representing the “noise” or incorrect  $\Lambda$  particle pairs. However, upon inspection there was no indication of the  $\Lambda$  peak. Thus, there were not enough correctly paired  $\Lambda$ s to create a visible bump in the data curve.

The process of reconstructing  $\Lambda$  and  $\bar{\Lambda}$  involved many methods of analysis. Such methods include distance of closest approach cuts, measuring track length, charge, momentum, and energy combinations of proton/ $\pi$  pairs to ensure that they originated from the same  $\Lambda$ . Several methods were used. First, several histograms were created to plot data from the tracks in each event as can be seen in figure 11. Each histogram was filled with data pertaining to each event. Next, via built in functions of the ROOT software some of the histograms were filled with their respective data (see figure 12 and 5d).

```

const Int_t      nbins      = 100      ;

histogram[0]    = new TH1F( "Vertex", "Event Vertex Z Position", nbins, -25.0, 25.0 ) ;
histogram[1]    = new TH1F( "Pt",  "Transverse Momentum for all particles", nbins, 0.0, 10.0 ) ;
histogram[2]    = new TH1F( "Px",  "X-component of momentum", nbins, -10.0, 10.0);
histogram[3]    = new TH1F( "KaonP", "Kaon momentum track", nbins, -10.0, 10.0);
histogram[4]    = new TH1F( "ProtonP", "Proton momentum track", nbins, -10.0, 10.0);
histogram[5]    = new TH1F( "PionP", "Pion momentum track", nbins, -10.0, 10.0);
histogram[6]    = new TH1F( "Charge", "Charge of each particle", nbins, -10.0, 10.0);
histogram[7]    = new TH1F( "RestmassLrange", "Rest mass of each particle", nbins, -10.0, 10.0);
histogram[8]    = new TH1F( "RestmassSrange", "Rest mass of each particle", nbins, 1.0, 1.2);

```

*Figure 11. Histograms to hold particle track data*

```

//For Tranverse Momentum
StMuTrack* track1 ;
while ( ( track1 = (StMuTrack*)GetTracks.Next() ) )
{
    histogram[1] -> Fill(track1->pt() ) ;

    histogram[2] -> Fill(track1->momentum().x() ) ;

    histogram[3] -> Fill(track1->nSigmaKaon() ) ;

    histogram[4] -> Fill(track1->nSigmaProton() ) ;

    histogram[5] -> Fill(track1->nSigmaPion() ) ;

    histogram[6] -> Fill(track1->charge() ) ;
}

```

*Figure 12. Filling the histograms with relevant information*

```

if(track1->nHitsPoss() >= 5 && (15<track1->nHits(<100))
{
    if(std::abs(Trackarr[i] -> nSigmaProton()) < 1.5)
    {
        if(Trackarr[i]->charge() > 0)
        {
            Protarrpos[j] = Trackarr[i];

            j++;
        }

        else if(Trackarr[i] -> charge() < 0)
        {
            Protarrneg[k] = Trackarr[i];
            k++;
        }
    }

    if(DCA > 1.5)
    {
        if(std::abs(Trackarr[i] -> nSigmaPion()) < 1.5)
        {
            if(Trackarr[i] -> charge() > 0)
            {
                Pionarrpos[l] = Trackarr[i];
                l++;
            }

            else if(Trackarr[i] -> charge() < 0)
            {
                Pionarrneg[m] = Trackarr[i];
                m++;
            }
        }
    }
}

i++;
}

```

Figure 13. Methods of narrowing the acceptable data

### 4.3 Momentum and Ionization Energy Loss (dE/dx)

Because there was a magnetic field applied at the moment of collision, we can determine the charge of the particle and its momentum. Specifically, in the presence of a magnetic field the positively charged protons will curve in a direction determined by the right-hand rule of the Lorentz Force, while the negatively charged  $\pi$ s will curve in the opposite direction. The radius of curvature in the field is determined by the momentum of the particle. Reference equations (2) - (6) to see how through algebraic manipulation, the radius of curvature of the particle  $\rho$ , and the momentum,  $P$  are related.

Starting from the base equation for Lorentz force, equation (1),

$$\vec{F} = q(\vec{E} + \vec{v} \times \vec{B}) \quad (2)$$

we can reduce to scalar quantities and get equation (4),

$$F = qvB. \quad (3)$$

A charged particle in a magnetic field will move in a circle or spiral. The equation relating the force to radius and velocity in constant speed circular motion is,

$$F = \frac{mv^2}{\rho} \quad (4)$$

Combining equations (3) and (4), we obtain,

$$\frac{mv^2}{\rho} = qvB. \quad (5)$$

By algebra, equation (5) reduces to equation (6)

$$mv = qB\rho = P \quad (6)$$

This leaves us with the equation relating  $\rho$  and  $P$ .

Energy loss is the amount of energy lost by the traveling particle over its distance traveled – which is generally a known value for the types of particles of interest that have passed through the TPC in this experiment. If this equation is broken down per variable it becomes much simpler to conceptualize. Ionization energy loss is represented by the Bethe-Bloch equation<sup>16</sup> (7) as follows:

$$-\left\langle \frac{dE}{dx} \right\rangle = \frac{4\pi}{m_e c^2} \cdot \frac{nz^2}{\beta^2} \cdot \left( \frac{e^2}{4\pi\epsilon_0} \right)^2 \cdot \left[ \ln \left( \frac{2m_e c^2 \beta^2}{I \cdot (1 - \beta^2)} \right) - \beta^2 \right] \quad (7)$$

*Bethe-Bloch Equation*

where  $E$  is the energy of a particle,  $x$  is the distance traveled, electron density  $n$  of target particles, excitation potential  $I$  (a known property of the gas),  $\beta = v/c$ , and constants the speed of light  $c$ , permittivity of free space  $\epsilon_0$ , rest mass of the traveling particle  $m_e$ , traveling particle charge  $z$ , and electron charge  $e$ . Disregarding constants, the only variable  $\beta$  is dependent on the velocity of the traveling particle. Therefore, in a sense, energy loss is a measure of the velocity of the traveling particle. This ionization energy loss has been roughly estimated through other experimental data. Figure 14 shows the histogram of expected energy loss curves of several common particles including the  $\pi$ , proton, electron, and the  $d$  meson. Other scientists have programmed methods within ROOT to determine the momentum and energy loss of each track and based off this, we decide which particle energy loss curve it best fits.

Implementation of this method works as follows. The ROOT software keeps a catalog of the average energy loss of the particles that have passed through, calculated from the resultant trail of electrons left behind. Therefore, by accessing the information stored for each track, we can compare the energy loss of each track to the energy loss of the other particles that have passed through. Finally, depending on which energy loss the track most closely resembles, we classify the track as either a proton or a  $\pi$ , or neither.

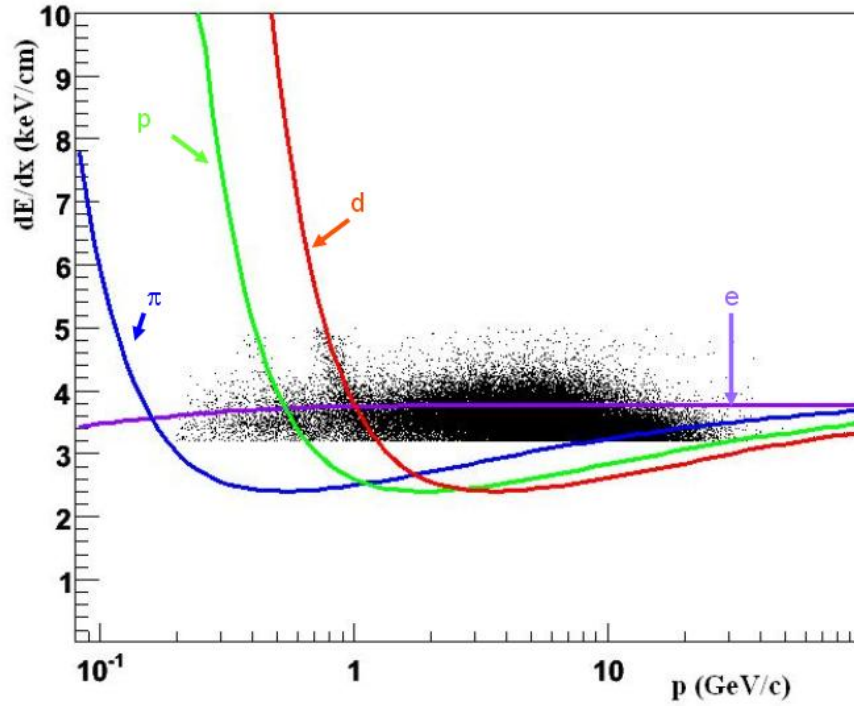


Figure 14. Plot of  $dE/dx$  - Ideal Ionization Energy Loss

#### 4.4 Track length cuts

Perpendicular to the drift direction is the pad plane. The pad plane consists of an anode segmented into numerous individual anode pads. Once the TPC gas particles are ionized and drifted towards the pad plane, a strong electric field is applied to amplify the electron signal from the ionization process. The TPC measures track length by the number of “pads” that interact with drifted charged gas particles. Track lengths are significant to the overall accuracy of the data.

There needs to be an acceptable upper track length in order to ensure the list of particles are not mistakes. If a track length is below a certain value, it is likely an error in the software’s pattern recognition or noise. We would expect the proton and  $\pi$  to cause  $\sim 5$  or more pads to be triggered. This is because the proton and  $\pi$  once decayed from the  $\Lambda$  should travel at least 5 pad lengths.

Therefore, we are able to remove any track with lengths shorter than that.

By using the ROOT identifier “nHitsPoss”, we access the value that represents the amount of pads triggered by a particular track. As can be seen in figure 13, through the use of *if* statements, any tracks shorter than the length of 5 pads is cut and provides a cleaner revised set of data to work with. This effectively means any particle that travels farther than what would be expected of a proton or  $\pi$ .

## 4.5 DCA Cuts

Distance of closest approach in this instance is essentially a measure of how far from the collision zone a particle originated. This is crucial to making data cuts because if any protons or  $\pi$ 's originated roughly at the collision zone or too far from the collision zone, they most likely are not daughters of a  $\Lambda$ , which typically travels a distance of a few centimeters before decaying into a  $\pi$  and  $\Lambda$ . If the particle's origins are determined by ROOT's algorithms to have come before the expected  $\sim 2\text{cm}$  distance from the collision point, then we can remove the protons and  $\pi$ s that originated from the collision itself and not from the decay of a  $\Lambda$  to improve the signal and decrease the noise. Thus, we can remove those tracks to ensure more accurate data. Figure 15 shows a diagram of the paths traveled by the  $\Lambda$ , proton, and  $\pi$ . The letters “PV” stand for “primary vertex” which essentially represents the collision zone of the Au+Au nuclei. As is shown, the proton and  $\pi$  decay is nearly opposite directions and are cut based on the distance of their origin from the primary vertex or collision zone.

The built-in function for calculating the distance of closest approach returns a three-vector which measures the overall length of the track in cm from the collision point to the last recorded drifted electron. Therefore, in order to make a real comparison between the distance the



track started and the acceptable distance at which a track can start, we needed to find the magnitude of the vector. Once found, we were able to use that value as one of the main comparison factors for narrowing the data. Figure 13 shows some of the implementation of the distance of closest approach method through use of *if* and *else* statements. This effectively cuts the particle tracks that began less than 1.5 cm from the collision zone.

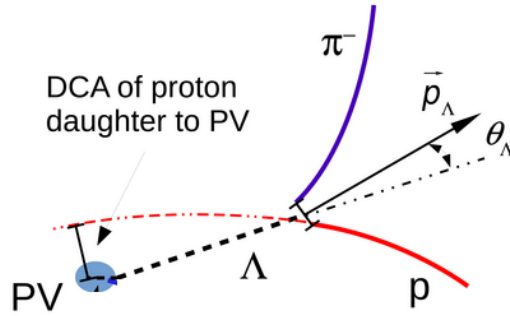


Figure 15. Diagram of  $\Lambda$  decaying into proton and  $\pi$

#### 4.6 Rest Mass and Total Energy

The momentum of each track was accessed by a built-in ROOT functions. As the particles move away from the primary vertex, they curve from the Lorentz force due to the applied magnetic field. Then, based on the curvature of the track and the strength of the B-field, ROOT calculates the momentum of each particle. Then by using the momentum, the following equation for rest mass was then rearranged to solve for energy – with the respective momentum value and expected mass for the proton/ $\pi$  pair plugged in<sup>17</sup>.

*Equation 8 Generic form of Invariant Mass*

$$m_0^2 c^2 = \left( \frac{E}{c} \right)^2 - \|\mathbf{p}\|^2 \quad (8)$$

We can remove the values of  $c$  because they will be used as part of the units for invariant mass ( $\text{MeV}/c^2$ ). Once the values of  $c$  are removed, then by simple algebra the equation for invariant mass becomes equation 2 for proton/ $\pi$  pairs.

*Equation 9 Equation for Invariant Mass without units of 'c'*

$$E_{Tot} = \sqrt{m_0^2 + p_{Tot}^2} \quad (9)$$

As can be seen, the form of equation 8 that we want is in terms of invariant mass and momentum, and what we're solving for is the total energy (the desired form is represented by equation (9)). That is, for each particle we want the total energy, and we already know the momentum and invariant mass. Because the protons and  $\pi$ s come in pairs to comprise the  $\Lambda$ s, it is vital to accommodate for the energy of both in the algebra. Once we have the energy for each particle in terms of mass and momentum we get the following equations:

*Equation 10 Total energy portion of invariant mass equation*

$$E_{Tot}^2 = p_{p,x}^2 + p_{p,y}^2 + p_{p,z}^2 + m_p^2 + p_{\pi,x}^2 + p_{\pi,y}^2 + p_{\pi,z}^2 + m_\pi^2 \quad (10)$$

*Equation 11 Total momentum portion of invariant mass equation*

$$P_{Tot}^2 = (p_{p,x} + p_{\pi,x})^2 + (p_{p,y} + p_{\pi,y})^2 + (p_{p,z} + p_{\pi,z})^2 \quad (11)$$

The code representing this algebra can be seen in figure 16. Each proton was paired with each  $\pi$

in order to create the histogram in figure 17, representing the rest mass of each combination.

The significance of this histogram is the peak (see figure 19). Figure 18 shows a zoomed in graph of the portion of figure 17 where we would expect to see a lambda peak.

Upon closer inspection of the code in figure 16, it can be seen that it is set up as a double for-loop to pair each proton with each  $\pi$ . This is significant because once plotted we hope to see a continuous slope aside from a sudden increase in frequency roughly at the value for the mass of a  $\Lambda$  (as seen in figure 12). This is the aforementioned  $\Lambda$  peak. The random combinations of  $\pi$ s and protons comprise the slope of the graph and represent incorrect pairs of protons and  $\pi$ s – while the peak represents actual correctly found  $\Lambda$  particles.

```
for(int i=0; i < numPosProt; i++)
{
    for(int j=0; j< numNegPion; j++)
    {
        Totel[j] = sqrt(pow(Protarrpos[i]->momentum().x(),2.0) + pow(Protarrpos[i]->momentum().y(),2.0) +
            pow(Protarrpos[i]->momentum().z(), 2.0) + pow(Protmass, 2.0)) + sqrt(pow(Pionarrneg[j]->momentum().x(), 2.0) +
            pow(Pionarrneg[j]->momentum().y(), 2.0) + pow(Pionarrneg[j]->momentum().z(), 2.0) + pow(Pionmass, 2.0));

        Totpl[j] = pow((Protarrpos[i]->momentum().x() + Pionarrneg[j]->momentum().x()), 2.0) + pow((Protarrpos[i]->momentum().y() +
            Pionarrneg[j]->momentum().y()), 2.0) + pow((Protarrpos[i]->momentum().z() + Pionarrneg[j]->momentum().z()), 2.0);

        Restmassarr1[j] = pow((pow(Totel[j], 2.0) - Totpl[j]), 0.5);

        histogram[7] -> Fill(Restmassarr1[j]);
        histogram[8] -> Fill(Restmassarr1[j]);
    }
}
```

*Figure16. Calculating the total energy and momentum for each  $\pi$  with each proton*

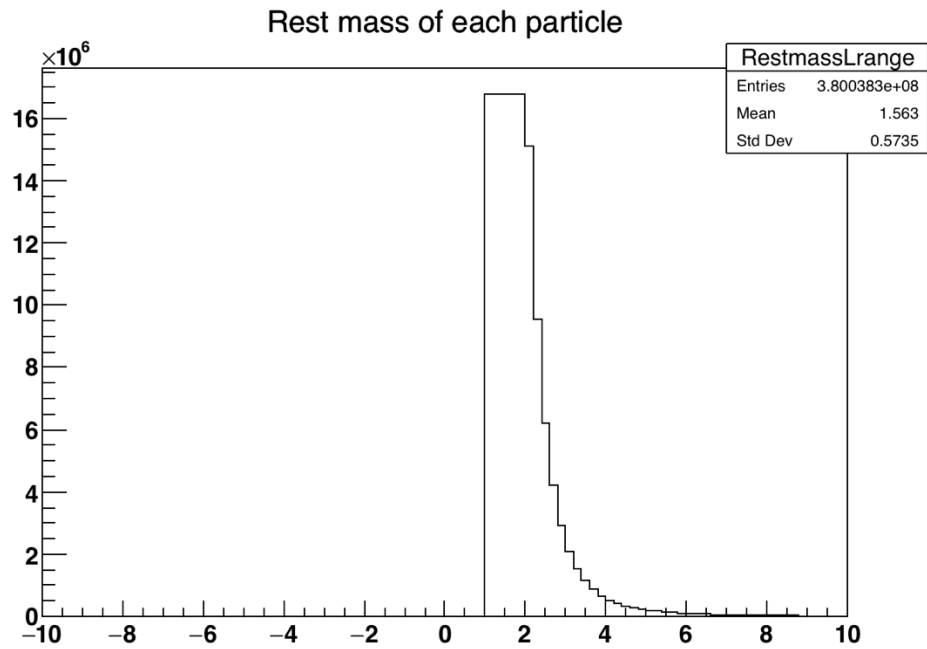


Figure 17. Wide range histogram of all combinations of rest mass

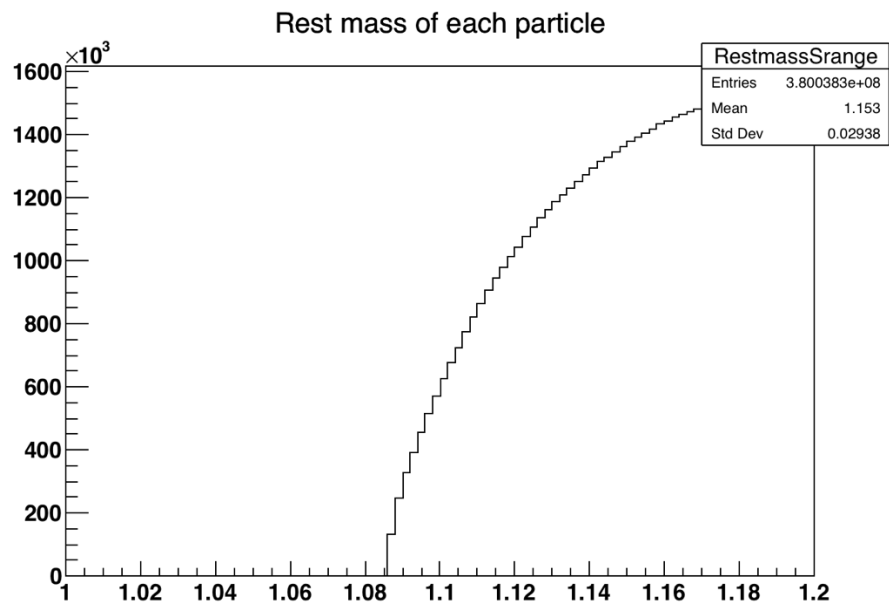


Figure 18. Small range histogram of all combinations of rest mass

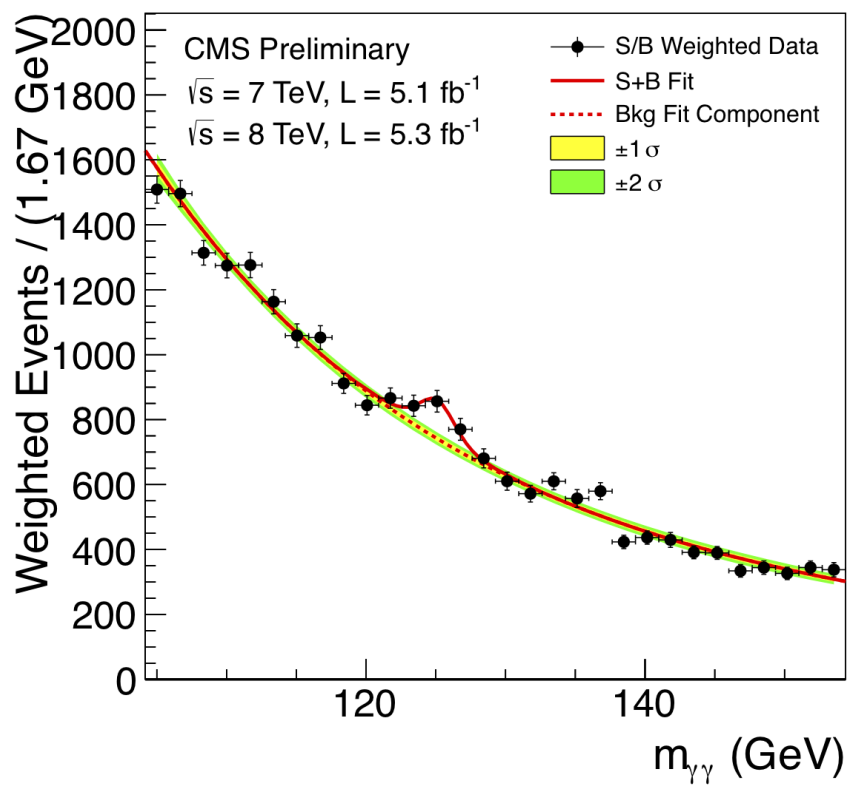


Figure 19. Example of histogram peak (not  $\Lambda$  particle)

## Results and Discussion

### 5.1 Not Actual $\Lambda$

The intended outcome of this research was to find  $\Lambda$  particles so that later work could examine their helicity in order to determine the existence of local parity violation. We intended to see a peak in the histogram at the value of the  $\Lambda$  mass. Ideally this peak would be a simple line peak, but due to the innate slight experimental imprecision of the instruments used in the experiment there would be an error associated with the peak called the instrumental width. This error would widen the ideal peak causing a similar visual as in figure 19. However, our findings resulted in no actual  $\Lambda$  peaks. Contrast figure 19 with figure 17. Figure 19 shows an ideal histogram peak around the mass of the particle of interest however, using data for a different experiment. Figure 17 shows the actual histogram we achieved through our data examination process. A key reason for not seeing an actual peak is a lack of available accessible data to determine a  $\Lambda$  peak from a histogram.

A peak in our histogram would indicate that the number of counts within a certain interval is at least a few times larger than the size of fluctuations in the number of background counts of the region of the histogram where the signal is found. Therefore, in order to increase the signal, we must also increase the the data size. It must be larger than the data size allowed by our default method of analysis within the ROOT software. The data size ceiling for our default method is  $\sim 5.0 \times 10^8$  entries, which corresponds to the 6500 max amount of events we were able to run. The amount of  $\Lambda$ s we expect to find per event is about 2. Multiply this value times the chances of finding a proton and  $\pi$ , together equaling 1%, leaving us with 0.02  $\Lambda$ s per event. The

histogram background noise equates to the square root of the number of counts within the range of where the  $\Lambda$  should appear.

Now, let's apply this information to our actual data. According to figure 9, because we would expect to see a peak between 1.110 and 1.120, the number of counts would be  $\sim(600 \times 10^3) \times 5 \cong 10^6$ . The square root of this value is about 1000. In conclusion, the number of  $\Lambda$ s we think is in the histogram is equal to the number of events multiplied by 0.02. If that number of  $\Lambda$ s is significantly larger than 1000, we would expect to see a  $\Lambda$  peak bump on top of the smoothly increasing background noise. Because our max number of events is 6500, it follows that the number of  $\Lambda$ s we should expect is 130. This value is significantly smaller than 1000 so we do not expect to see a  $\Lambda$  peak, and as the histogram shows we do not.

## 5.2 Success

Overall, what we achieved in this work was a baseline framework that can be used for analyzing STAR data. The first obstacle overcome was gaining access to the data via remote access. The STAR data lies behind several verifications and trainings, and thus took a decent amount of time to gain access to. Once the data was obtained, each track was separated into two subcategories; protons and  $\pi$ s. Once separated, the data was further cut via the distance of closest approach method which proved quite useful. In conclusion, the key result was the base sorting of likely particle candidates and remote access. The experiment gave us insight into roughly how much more data we need access to in order to complete the experiment and whether it is likely that we will be able to derive the  $\Lambda$  peak. This research lays the foundation for the next steps.

### 5.3 Next Steps

The next steps toward the completion of this research is to get more data. The current level of data cuts has provided a useful framework for a baseline of fairly accurate data to work with. However, there are more data cuts that can be made. For example, further manipulating the signal so that we are left with conclusions with stronger statistical support. The signal can be improved by being more selective about which protons and  $\pi$ s are used. Another important piece to note is the amount of track and track information we were able to work with. Because there was a limit to the amount of data in formats easily accessible that we were able to access by our methods, it caused us not to be able to create the  $\Lambda$  peak histogram as desired.

In order to determine the amount of events necessary to see an actual  $\Lambda$  peak, we first need to find the number of events  $N$  such that the number of signal counts is at least three times larger than the background noise (which is the square root of the number of background counts). If  $signal = N * (2 \Lambda \text{ per event}) * (0.1 \text{ chance to find } \pi \text{ per event}) * (0.1 \text{ chance to find proton per event}) = 0.02 * N$  and  $noise = \sqrt{N * (10^6 \text{ entries}) / (6500 \text{ events})} = \sqrt{153.85 * N}$ , we want to find  $N$  such that  $signal = 3 * noise$ . Thus we are left with  $0.02 * N = 3 * \sqrt{153.85 * N}$ , which equates to  $N = 3,461,538$  events.



## References

- 1: Heavy ions and quark-gluon plasma. (n.d.). Retrieved April 11, 2017, from <https://home.cern/about/physics/heavy-ions-and-quark-gluon-plasma>
- 2: " The Physics of RHIC. (n.d.). Retrieved May 23, 2017, from <https://www.bnl.gov/rhic/physics.asp>
- 3: Examples of particle interactions described in terms of Feynman vertices. (n.d.). Retrieved April 15, 2017, from <http://hst-archive.web.cern.ch/archiv/HST2002/feynman/examples.htm>
- 4: Working Principle of a TPC. (n.d.). Retrieved May 3, 2017, from <https://www.lctpc.org/e8/e57671/>
- 5: Fall of Parity Conservation. (n.d.). Retrieved April 17, 2017, from <https://www.aps.org/publications/apsnews/200112/history.cfm>
- 6: Bzdak, A., Koch, V., & Liao, J. (2011). Azimuthal correlations from transverse momentum conservation and possible local parity violation. *Physical Review C*, 83(1).  
doi:10.1103/physrevc.83.014905

7: Orwig, J. (2012, October 10). Time projection chambers: a milestone in particle detector technology. Retrieved May 18, 2017, from <https://www.symmetrymagazine.org/article/october-2012/time-projection-chambers-a-milestone-in-particle-detector-technology>

8: Hegstrom, R. A., & Kondepudi, D. K. (1990). The Handedness of the Universe. *Scientific American*, 262(1), 108-115. doi:10.1038/scientificamerican0190-108

9: The Physics of STAR. (n.d.). Retrieved May 11, 2017, from <http://www.star.bnl.gov/central/physics/>

10: Anderson, M., Berkovitz, J., Betts, W., Bossingham, R., Bieser, F., Brown, R., . . . Zhang, W. (2003, January 27). The STAR Time Projection Chamber: A Unique Tool for Studying High Multiplicity Events at RHIC. Retrieved May 5, 2017, from <https://arxiv.org/abs/nucl-ex/0301015>

11: Anderson, M., Berkovitz, J., Betts, W., Bossingham, R., Bieser, F., Brown, R., . . . Zhang, W. (2003, January 27). The STAR Time Projection Chamber: A Unique Tool for Studying High Multiplicity Events at RHIC. Retrieved May 5, 2017, from <https://arxiv.org/abs/nucl-ex/0301015>

12: Griffiths, D. J. (2014). *Introduction to elementary particles*. Weinheim: Wiley-VCH Verlag.

13: Lorentz Contraction. (n.d.). Retrieved March 19, 2017, from  
<http://www1.phys.vt.edu/~takeuchi/relativity/notes/section13.html>

14: Working Principle of a TPC. (n.d.). Retrieved May 3, 2017, from  
<https://www.lctpc.org/e8/e57671/>

15: “Working Principle of a TPC. (n.d.). Retrieved May 3, 2017, from  
<https://www.lctpc.org/e8/e57671/>

16: CHARGED PARTICLE INTERACTIONS. (n.d.). Retrieved April 23, 2017, from  
<http://www.med.harvard.edu/JPNM/physics/didactics/physics/charged/lect.html>

17: Wong, C. (1994). *Introduction to high-energy heavy-ion collisions*. Singapore: World Scientific.